Unmanned Aerial Systems in Remotely Sensed Biomass Estimates: How they Improve the Quality of Existing Satellite Based Approaches

Leon **GAW** Yan Feng

Academic exercise submitted in partial fulfilment of the requirements for the degree of:

Master of Science in Geospatial Technologies

Institute for Geoinformatics

2018

Declaration

I wrote this thesis on my own without the help of others, listed all used references and sources, and that did not submit this thesis to any other university.

Leon GAW Yan Feng

Münster, 15 February 2018

Name:	Leon GAW Yan Feng
Matric. Number:	447201
Email:	l_gaw001@wwu.de
Hosting university:	University of Münster (WWU)
Supervisor:	Torsten PRINZ (WWU)
Co-supervisor 1:	Jan LEHMANN (WWU)
Co-supervisor 2:	Ignacio GUERRERO (UJI)

Unmanned Aerial Systems in Remotely Sensed Biomass Estimates: How they Improve the Quality of Existing Satellite Based Approaches

Leon Y.F. Gaw[1]
[1]Institute for Geoinformatics, University of Münster, Germany

Correspondence: Leon Y.F. Gaw (e-mail: l_gaw001@wwu.de)

Abstract

Forests of the world provide an important ecosystem service in the fight against climate change by sequestering carbon from the atmosphere and storing them as biomass. However, cloud cover and terrain inaccessibility hamper studies of forest biomass using satellites, especially in the dense jungles of the tropics. This study investigated the use of UAS to complement existing satellite based approaches by exploring what information can be derived from UAS sensors and how their biomass estimates can be applied to satellite sensors to improve their accuracies. A biomass estimation model was built using on the ground measurements while GIS was used to generate biomass maps. The results from the model show that NDVI and tree heights were statistically significant explanatory variables for biomass in the Mixed Oak Forests of Davert, Germany. Estimates from UAS were the most accurate in terms of R^2, compared to other sensor estimates from Sentinel 2, World View 3 and Orthophotos. Hence, two adjustment factors were proposed to improve the accuracy of World View 3 and Sentinel 2 estimates. UAS are thus a versatile sensor platform for biomass studies that complements satellite sensors to improve studies of global biomass of forests.

Keywords: biomass, drones, modelling, Sentinel 2, UAS, vegetation indices, World View 3

1 Introduction

Forests of the world are sentinel ecosystems that contain a rich variety of flora and fauna (Steffan-Dewenter *et al*., 2007). Although there are many different types of forest biomes, a common ecosystem service they provide to humans, on a global scale, is their ability to sequester carbon from the atmosphere to produce biomass via photosynthesis (Lal, 2004), which is stored in trees' stem, branches, leaves, and roots (Goulden *et al*., 1996). This ecosystem service of forests is important to regulate carbon and its gaseous compounds, which are potent greenhouse gases, in the earth's atmosphere. Unfortunately, carbon release into the atmosphere is far outpacing carbon absorption by forests that results in the present human-induced climate change (Oreskes, 2004). Therefore, the estimation of forest biomass on the earth's surface is important in understanding how much carbon is stored within and, when

combined with studies related to primary productivity of trees (Scurlock *et al*., 2002), the carbon fluxes between them and the earth's atmosphere.

The most accurate estimate of forest biomass comes from field measurements of trees' volume and density of their wood (Catchpole & Wheeler, 1992). Volume can be estimated by species (seldom forests) specific allometric equations that take into account a tree's diameter-at-breast height (DBH) and sometimes its height to model its volume (Yang *et al*., 2017). Density is estimated by destructive sampling techniques ranging from falling an entire tree or obtaining a core of its wood to be processed in a laboratory and obtaining density estimates from them (Brown *et al*., 1989). Thus, the product of a tree's volume and density would be its biomass. However, field sampling of biomass across large areas of forest is impractical due to the costs in terms of time and resources. This is impossible in some situations due to terrain inaccessibility and dense forests that make fieldwork dangerous (Cárdenas *et al*., 2017). To overcome these limitations and estimate biomass for large areas, albeit at the expense of estimation accuracies, researchers have turned to remote sensing techniques used for studies of the earth's surface.

To estimate forest cover and therefore biomass, existing remote sensing approaches rely heavily on spectral imagery captured by spaceborne satellites (Eckert, 2012). These sensors detect the spectral reflectance of sunlight from trees, for example, and maps of forest cover can be generated from this data. However, the spatial resolution of images from spaceborne sensors are coarse, especially in studies of forests on regional and global scales (Avitabile *et al*., 2012). Furthermore, validation of classified land cover maps with on the ground measurements is vital to evaluate the accuracy of maps (Congalton, 1991), and such measurements are sometimes difficult to obtain. Another difficulty of capturing satellite images in the tropics is the problem of cloud cover that obscures the earth's surface below it, especially near the equator. One solution to this is to fill in the gaps to the data because of cloud cover by mosaicking images of the same area but captured on a different date (for example in Pettorelli *et al*., 2005). This is not ideal if the study has a temporal element in its analysis. Thus, a new sensor platform is needed to not only operate under cloud cover and in challenging terrain, but also produce more accurate biomass estimates compared to satellite estimates to validate them as a replacement to on the ground measurements.

Unmanned aerial systems (UAS) are increasingly used in geographical research, especially in the fields of land cover and forest ecology (Yue *et al*., 2017). Sensors, more often an image capturing device, are attached to UAS (also known as drones), and are flown over a

study area to capture geotagged images or videos. Thereafter, the geotagged data are processed in a geographic information system (GIS) to create maps of the study area. The use of UAS makes acquisition of geographical data convenient as they can be flown at low costs anytime and anywhere, subject to the weather and prevailing rules and regulations of the study locale (Clarke & Moses, 2014). An added benefit of UAS is that they can be flown below the cloud line to capture images of the earth's surface that makes them an ideal solution to cloud obscurity to satellites, particularly in the tropics.

UAS can not only capture high resolution multispectral imagery, but also generate point clouds based on imagery overlap that can be translated into three-dimensional (3D) objects of, for example, trees, using image processing software (Rosskopf *et al*., 2017). This combination of multispectral imagery, useful in calculating vegetation indices, and 3D models of forests, useful in calculating heights and volumes, are key in estimating forest biomass. Before the use UAS, point clouds were captured using Light Detection and Ranging (LiDAR) sensors mounted on board airplanes. Such flights are not only expensive (Popescu, 2007), but also limits the area of interest as there are restrictions to the flight paths of airplanes, especially in urban areas. UAS have thus emerged as a convenient solution to airborne flight limitations as their ability to capture and derive point clouds based on imagery to generate 3D models makes them useful in biomass estimation that requires volume estimates of trees in a study area.

From the context and literature introduced, this study aims to investigate the role of UAS in improving the quality of existing satellite-based approaches. Two main research questions guide the aim of this study:

1. How are UAS of use in biomass studies?
2. How can UAS improve satellite biomass estimates quantitatively?

2 Methods

This section describes how data collected in the Davert, a temperate forest in Germany, was translated into the results of a biomass estimation model for the UAS and maps of biomass in the study area. Two methods were employed to estimate biomass, first using satellite sensors and published biomass equations. Second, a biomass model was built specifically for the UAS in the context of Davert as no published biomass models suited the radiometry of the sensors flown on the UAS.

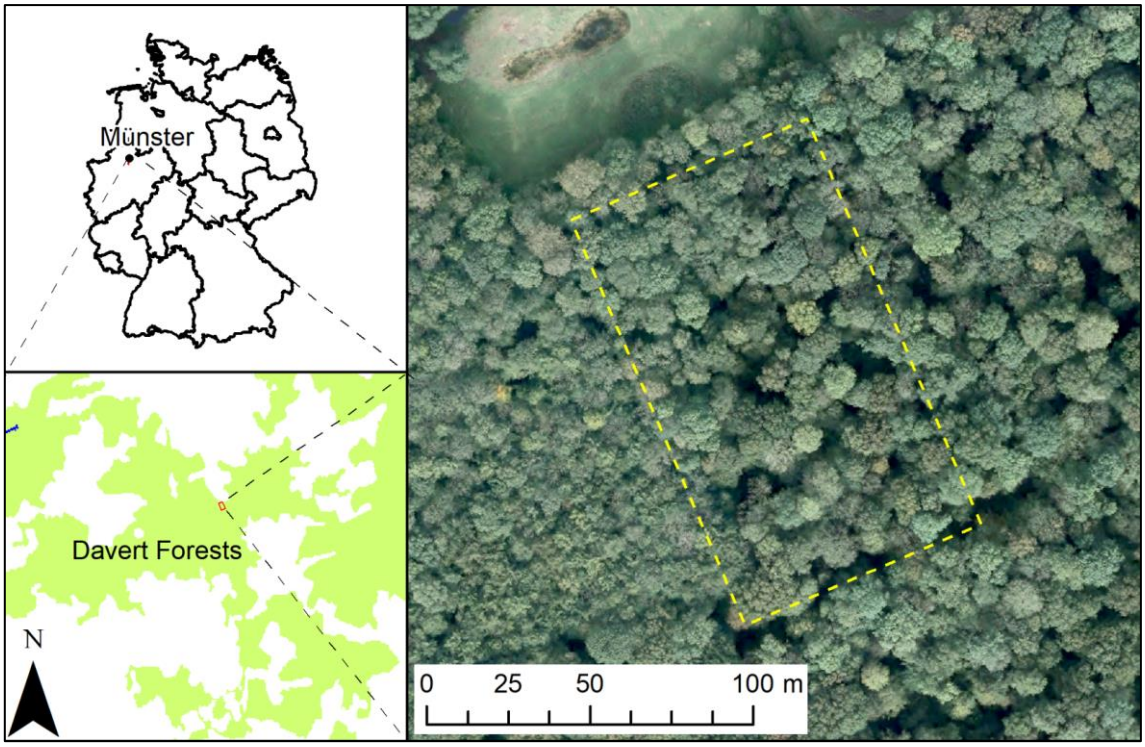

Figure 1: *Map of Davert south of Münster city where this study is situated. The dashed yellow line outlines the study area measuring 78 by 135 m where data was collected.*

2.1 Study area

Davert is a forested area in central Münsterland and it lies between the city of Münster (to its north), the municipalities of Senden (to its west), and Ascheberg (to its south). The total area of Davert is more than 2,500 ha (NABU, 2017) and spread throughout the Münsterland, with forest pockets linked together by parks and green corridors. The forest biome of Davert is considered a Mixed Oak Forest (Lehmann, pers. comm., 2017), typical of the Münsterland, made up of species like Oak (*Quercus robur*), Ash (*Fraxinus excelsior*), Elm (*Ulmus laevis*), Hazel (*Corylus avellana*), and Hornbeam (*Carpinus betulus*) (NABU, 2017). The study area was a 1.06 ha rectangular patch of forest, measuring 78 by 135 m, with the centroid located at Easting 403,001.42 and Northing 5,745,539.74 (UTM Zone 32U), in the northern reaches of Davert (Figure 1).

2.2 Remote sensing data and processing

Data for this study were all downloaded from secondary sources. Since the study began in the autumnal month of September, the foliage of trees were beginning to decrease and UAS flights then would not show maximum green foliage of trees (used for photosynthesis) that was important for investigating their biomass.

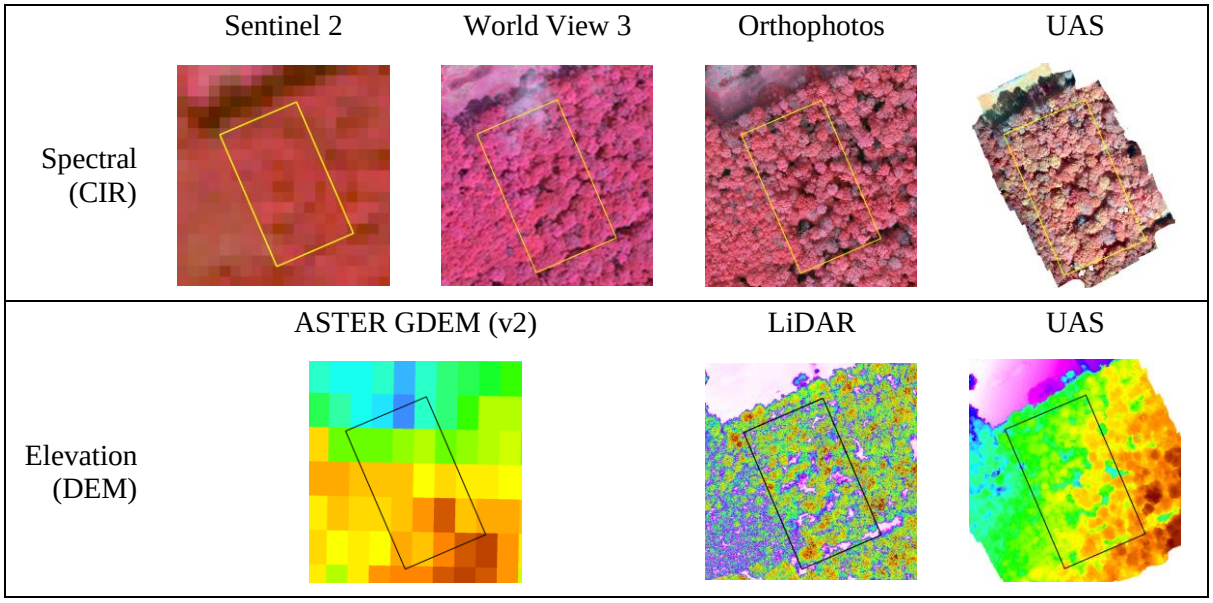

Figure 2: A *comparison of the spatial resolution of sensors used for biomass estimation from the lowest on the left to the highest on the right for spectral and elevation data.*

Table 1: *Technical specifications of the sensors used in this study. Source: ESA (2017), DigitalGlobe (2014), Vexcel Imaging (2016), Tetracam Inc. (2017).*

Platform	Sensor	Spectral Bands	Spatial Resolution (m)	Temporal Resolution (days)	Spectral Range (µm)	Date Acquired
Sentinel 2 (Satellite)	Multi Spectral Instrument (MSI)	4	10	16	0.40–0.98	25092016
World View 3 (Satellite)	Multi Spectral	8	1.2	<1	0.40–1.04	16062015
Aircraft (Airborne)	Ultra Cam Eagle	4	0.2	Flight dependent	0.41–1.00	08032016
Microdrones MD 4-1000 (UAS)	Tetracam Mini-MCA	5	0.2	Flight dependent	0.53–0.92	18082016

The four sources of remotely sensed spectral images of the study area were from, in ascending order of spatial resolution, Sentinel 2 (Copernicus, 2016), World View 3 (provided courtesy of the DigitalGlobe Foundation), Orthophotos (Geoportal NRW, 2017a), and UAS (Figure 2). The specifications of each sensor system are described in table 1. In addition to spectral images, elevation data used to supplement biomass estimates from the spectral sensors were from ASTER Global Digital Elevation Model (GDEM) version 2 (NASA LP DAAC, 2015) for the satellite sensors, and airborne LiDAR (Geoportal NRW, 2017b) flown separately from the Orthophotos flight.

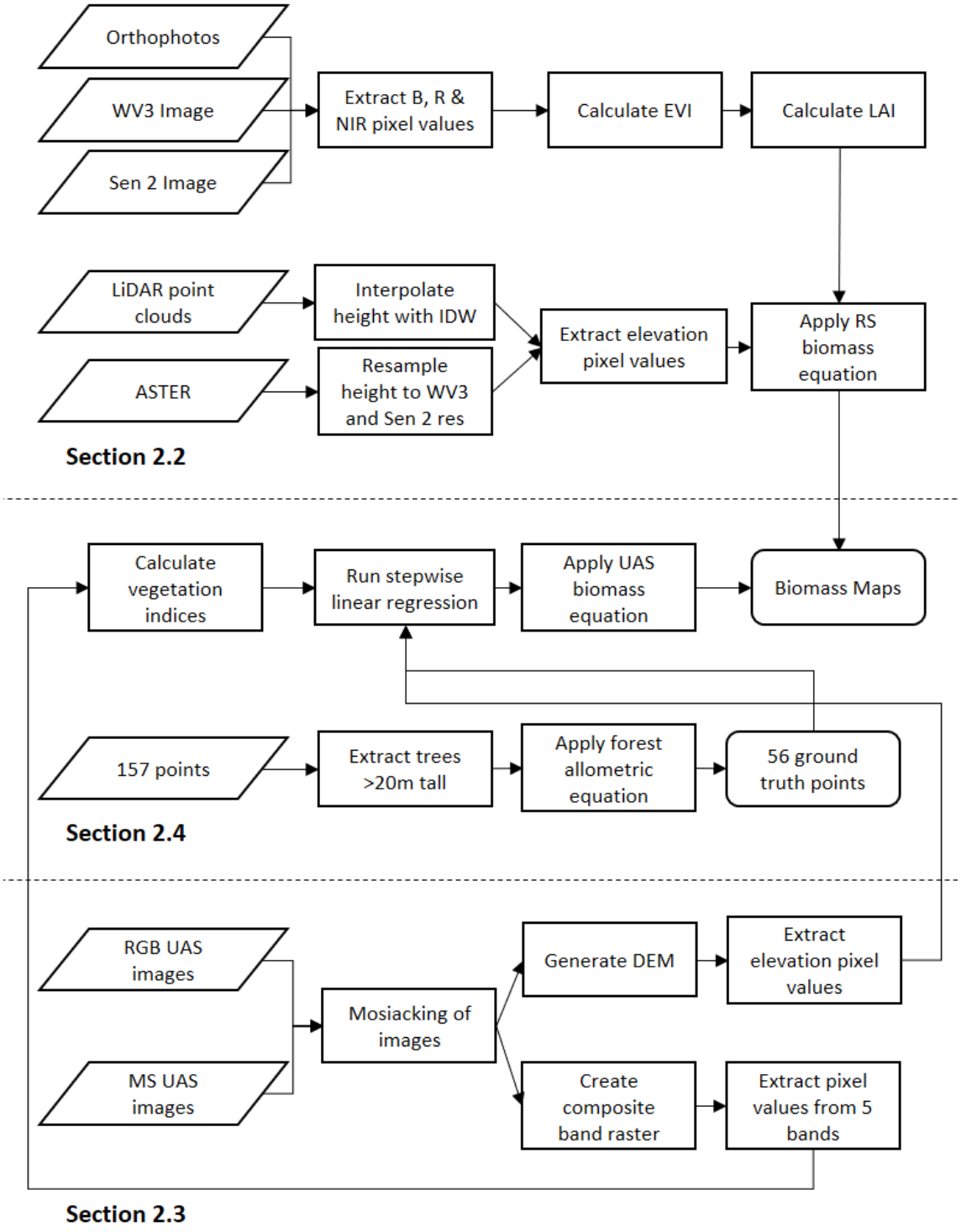

Figure 3: *Flowchart illustrating the methods described for (from top to bottom) remote sensing processing, biomass modelling and UAS processing. The final product are biomass maps derived from the four different sensors.*

To estimate forest biomass with remote sensing, researchers have used a combination of vegetation indices and elevation data (Castillo *et al*., 2017; Yue *et al*., 2017; Jachowski *et al*., 2013). In the context of this study, the equation published by Castillo *et al*. (2017) to estimate biomass with vegetation indices and elevation was most suited to the spectral signatures that Sentinel 2, World View 3, and Orthophotos detect. This was because they three captured the spectral bands of Blue, Red and Near Infrared (NIR) used in deriving vegetation indices related to biomass (Table 2). The model is represented by the equation (Castillo *et al*., 2017):

$$Biomass = 7.47 * LAI + 9.30 * Elevation - 16.07 \quad (1)$$

In the equation, the vegetation index used was the Leaf Area Index (LAI) (Boegh *et al*., 2002) derived from the Blue, Red and NIR pixel values of the three different sensors that first calculated the Enhanced Vegetation Index (EVI) (Huete *et al*., 2002) before the LAI. The elevation data used for Sentinel 2 and World View 3 calculations was from ASTER GDEM while the Orthophotos were paired with LiDAR point clouds. The pixel size of ASTER GDEM (15 m) was resampled to the pixel size of 10 m for Sentinel 2 and 1.2 m for World View 3 using cubic interpolation. The elevation recorded by point clouds from the LiDAR flight was interpolated using Inverse Distance Weighting (IDW) to obtain the DEM from LiDAR with a pixel size of 0.2 m. The methods described in this section (2.2) can be summarised in the top third of the flowchart in figure 3, which also details the methods described in sections 2.3 and 2.4.

2.3 UAS data and processing

The UAS used to survey the study area was the Microdrones MD 4-1000. Two separate flights were flown, one to capture multispectral images of the study area using a Tetracam Mini-MCA fitted with five spectral sensors (Table 1); and the other to capture RGB images of the study site using a Canon PowerShot SD780 camera. AgiSoft Photoscan software (AgiSoft, 2016) was used to mosaic the images to of the study site. Thereafter, a composite layer of five bands was created for the multispectral images, while point clouds of heights in the study area was generated using RGB images. Although point clouds could be generated from the mosaicked multispectral images, the RGB image was preferred for point cloud generation since the Canon camera has a global shutter mechanism that captures better quality images, which when mosaicked together, renders a smoother image of the entire study area and hence, more accurate point clouds of heights.

The outputs of AgiSoft Photoscan were a composite raster of five multispectral images, and a DEM of the study area created from RGB images. These two rasters were projected to the coordinate system of ETRS 1989 (UTM Zone 32N) so that length and area measurements can be made. Finally, the rasters were exported as a tagged image file format (tif) to ArcGIS Desktop 10.5 (ESRI, 2016) for processing with GIS.

2.4 Biomass estimation models with stepwise regression

To estimate forest biomass from the multispectral images and DEM of the UAS, a model specific to the use of the UAS in Davert was built using a stepwise linear regression (suggested by Jachowski *et al*., 2013). Data used to train this model was obtained from NABU's field survey of Davert (Area AU3) in 2014 that recorded trees' genus, species, DBH, and height (Table A1). These data were sufficient in generating biomass estimates based on the forest specific allometric equation from (Wang, 2006) (instead of species-specific ones) that was applicable to the temperate forest of Davert. Only trees with heights of the study area's median of 20 m and above were used to train the model, as the assumption was that only trees of such heights were captured by a UAS flown above. Hence, 157 tree measurements were reduced to 56 for model building. The allometric model that uses DBH to estimate biomass is represented by the equation (Wang, 2006):

$$\log_{10} Biomass = 1.95 + 2.47 * \log_{10} DBH \quad (2)$$

The pixel values of the five multispectral bands and DEM from the two mosaicked raster files were extracted from locations of the 56 tree measurement points. Thereafter, vegetation indices calculated from the five spectral signatures available were derived using the equations listed in table 2.

Before running the stepwise regression model, correlations amongst variables were checked using a correlation matrix generated by Microsoft's Data Analysis Tool Pack. From this matrix, variables were checked for correlation strengths with biomass, and whether the direction of correlations makes sense in relation to biomass. Next, a stepwise regression using the said Tool Pack was ran where explanatory variables of biomass were selected based on the directions of their coefficients and their statistical significance. The overall model's performance was evaluated by its coefficient of determination (R^2), a measure of the proportion of variance in biomass estimated that can be predicted by the explanatory variables.

Table 2: *Selected vegetation indices derived from spectral sensors in biomass model building plus tree height. Indices beginning with 'M' mean that the reflectance of the Green band was used in calculating indices instead of Blue as suggested by their respective reference.*

Variable name	Variable definition	References
Tree Height	From DEM	Yang *et al*., 2017
Vegetation Indices		
M*(Modified)ARVI	$\frac{NIR - 2 * Red + \boldsymbol{Green}}{NIR + 2 * Red - \boldsymbol{Green}}$	Kaufman & Tanré, 1992
M*EVI	$2.5 * \frac{NIR - Red}{NIR + 6 * Red - 7.5 * \boldsymbol{Green} + 1}$	Huete *et al*., 2002
IPVI	$\frac{NIR}{NIR + Red}$	Crippen, 1990
LAI	$3.6 * EVI - 0.1$	Boegh *et al*., 2002
NDVI	$\frac{NIR - Red}{NIR + Red}$	Rouse *et al*., 1973
M*OSAVI	$\frac{NIR - Red}{NIR + Red + \boldsymbol{Green}}$	Rondeaux, 1996
Simple Ratios		
RVI	$\frac{NIR}{Red}$	Jordan, 1969
NIR over Green	$\frac{NIR}{Green}$	
GRVI	$\frac{Green}{Red}$	Kanemasu, 1974

Note: Red in the equations above might be from the Red or Red Edge band. Similarly, NIR can be from NIR 1 or NIR 2 of the Tetracam Mini-MCA.

3 Results

This section describes the results of the biomass estimation model developed specifically for the UAS in the context of Davert and the resultant biomass maps produced from UAS data and the three other sensors. The comparisons show that there are not just differences in the accuracy of the estimates measured by models' R^2, but also the spatial variations of the estimates shown in the maps.

3.1 Biomass model for UAS data

From the correlation matrix (Table 3), vegetation indices calculated with the Red Edge and NIR 1 spectral band of the UAS have the highest positive correlation with biomass compared to indices from other combinations of Red and NIR 2. For an iteration of the model that used the latter two bands, please see supplementary figure A2.

Table 3: *Correlation matrix of explanatory variables and biomass. Values indicating high correlations with one another are italicised while variables in the second column marked with an asterisk are those used in the stepwise regression.*

	Biomass	Height	MARVI	MEVI	IPVI	NDVI	MOSAVI	RVI	N/G	GRVI
Biomass	**1**									
Height	0.39*	**1**								
MARVI	0.26*	0.02	**1**							
MEVI	-0.20	-0.03	0.05	**1**						
IPVI	0.23	0.06	0.59	-0.05	**1**					
NDVI	0.23*	0.06	0.59	-0.05	*1*	**1**				
MOSAVI	0.17	0.07	0.38	-0.07	*0.97*	*0.97*	**1**			
RVI	0.15	0.13	0.35	0.00	*0.81*	*0.81*	*0.85*	**1**		
N/G	0.01	0.07	-0.05	-0.07	0.70	0.70	*0.85*	0.79	**1**	
GRVI	0.27*	0.09	*0.89*	0.08	0.57	0.57	0.39	0.54	0.00	**1**

Model equation

$$Biomass = 100.12 * NDVI + 1.57 * Height - 38.62$$

p value of:	
Model	<0.01
Tree Height	<0.01
NDVI	0.01
multiple R	0.49
R^2	0.24
Adjusted R^2	0.21
VIF	1.32

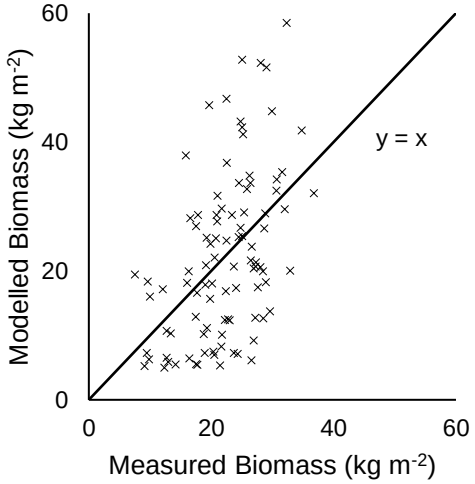

Figure 4: *Generated model and statistics for biomass with chart output. NDVI, a measure of vegetation greenness and Tree Height were selected by the stepwise regression as explanatory variables for biomass.*

Tree height, estimated by the DEM has the highest positive correlation with biomass. The correlation matrix also helps identify explanatory variables that were highly correlated with each other, defined in this study as those with an absolute correlation value of more than 0.8. With confounding explanatory variables that had little correlation with biomass removed, the remainder of the explanatory variables were used in the stepwise regression and the formula of the resultant biomass estimation model was a function of tree height and the Normalised Differentiated Vegetation Index (NDVI). The model had a statistically significant F value with the p value of it being less than 0.01, while the two explanatory variables were also statistically significant, both having p values of less than 0.05. However, the R^2 statistic of the regression

model was low at 0.24 (Figure 4). Its Variance Inflation Factor was low at 1.32 that showed low multicollinearity in the model. Hence, this model generated was the most suitable from the training data available to create a biomass estimation map of the study area based on UAS data.

3.2 Relative biomass maps

The following description focuses on the results shown in figures 5 and 6. Overall, the biomass estimates produced by the model in figure 4 using UAS data produced the highest accuracy (measured by the R^2) in biomass estimates in kg m^{-2}. Additionally, the resampled UAS data to the satellites' resolution of 10 m and 1.2 m for Sentinel 2 and World View 3, respectively, still shows higher accuracies compared to measurements from only satellites. The following paragraphs provides a more detailed comparison of UAS estimates to the three other sensor systems used in this study.

UAS vs Orthophotos: Before UAS, images of forests at sub-meter resolutions were acquired from aerial photography like Orthophotos. Hence, this comparison serves to benchmark UAS biomass estimates with Orthophotos (plus LiDAR for elevation). The Orthophotos produced a more even spread of biomass estimates across the study area while the estimates from the UAS show more biomass in the south and less in the north. The contrasts amongst pixels of biomass estimates from the UAS were also sharper where tree canopies show high biomass and the adjacent forest floor showing low biomass. The scatterplots show that biomass estimates from the Orthophotos under-estimated biomass of the study area since most of the points fell below the line of perfect correlation, an indication that measured biomass were more often higher than modelled biomass.

UAS vs World View 3: The second comparison is of UAS to high-resolution satellite data from World View 3. The biomass estimates from World View 3 were made in conjunction with a separate ASTER GDEM elevation data that had a coarser pixel size than World View 3 (15 m compared to 1.2 m). After resampling, the patterns of biomass in the study area still appeared similar to the original UAS image. The World View 3 biomass estimates were more pocketed with gaps in the canopy versus the resampled UAS estimates. Moreover, the low estimates of biomass in the north was shown in the World View 3 map as with the resampled UAS map. The R^2 of the scatterplot showed that the biomass estimated by World View 3 was the least accurate at 0.07 amongst the six maps and there was no discernible correlation between the modelled and measured biomass.

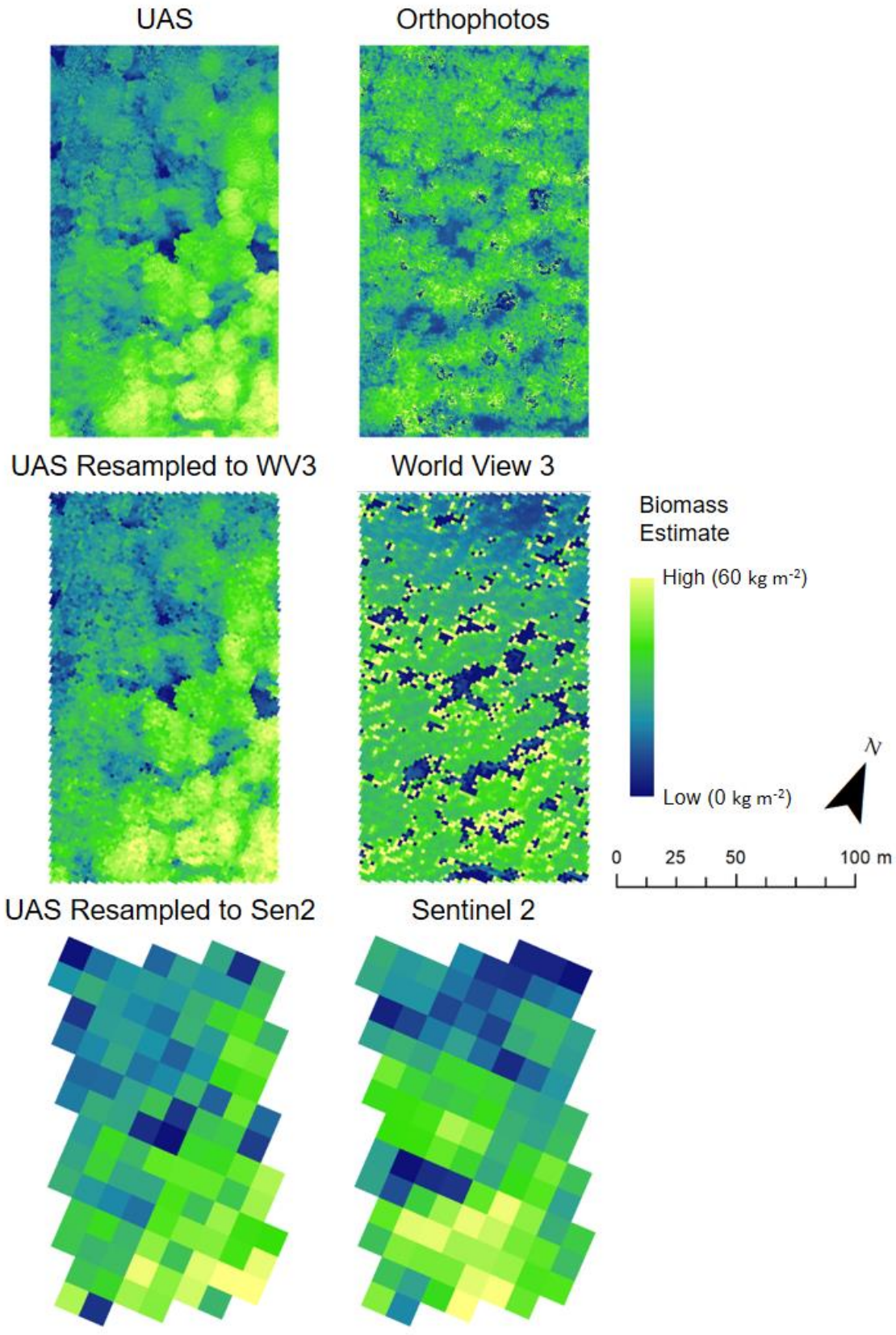

Figure 5: *Maps of biomass estimates from the different sensors. The comparison here focuses on the spatial variations of estimates.*

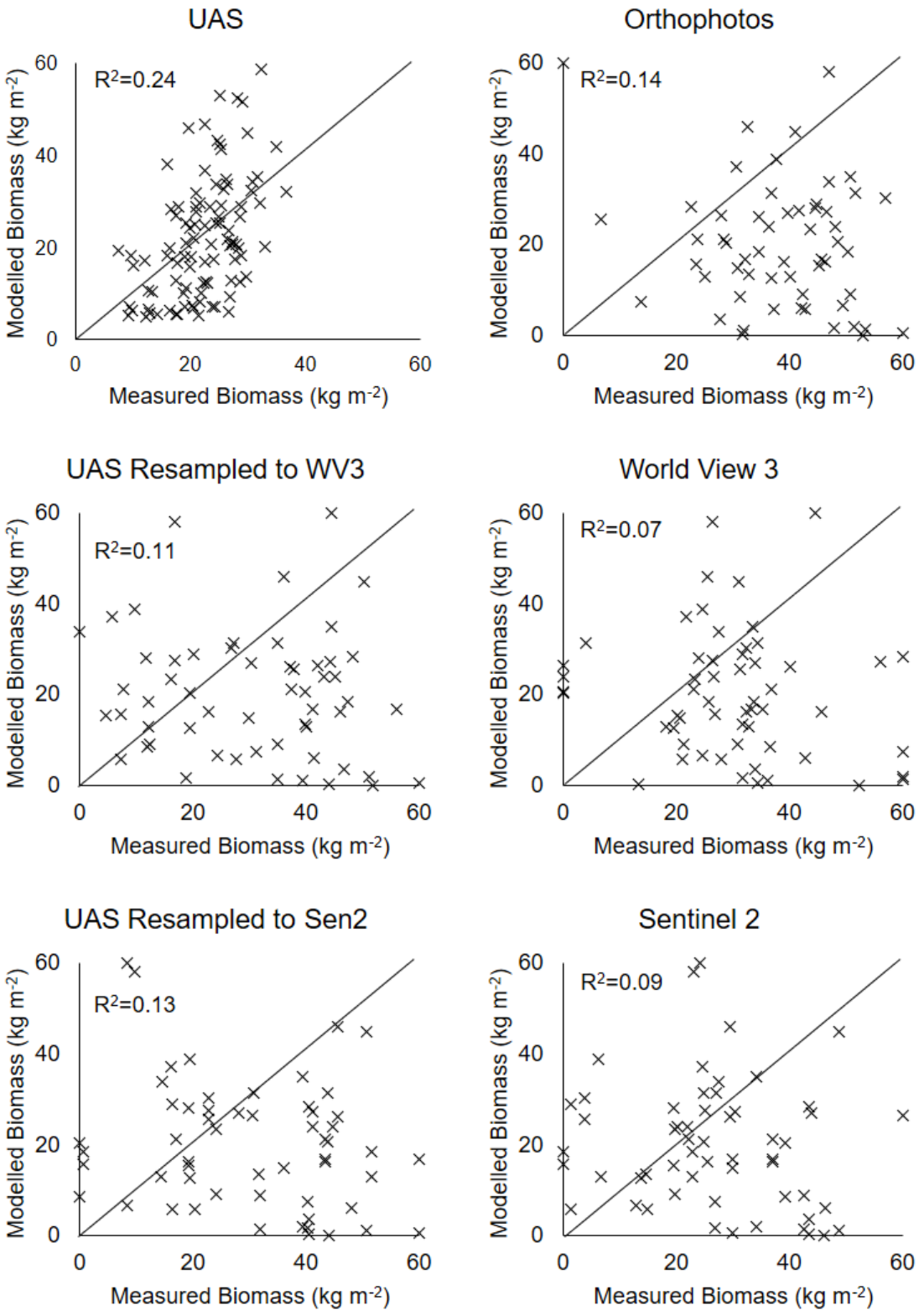

Figure 6: *Scatterplots of biomass estimates from the four different sensors. The comparison here focuses on the accuracy of relative (high-low) biomass by this study's biomass model applied to the UAS and Castillo et al.'s (2017) model applied to the other three sensors.*

UAS vs Sentinel 2: The third comparison is of UAS to the medium resolution satellite of Sentinel 2 used for areal studies from regional to global scales. Elevation data was also obtained separately from ASTER GDEM. The resampled UAS image to the resolution of Sentinel 2 looked the most similar to Sentinel 2's estimate amongst the three comparisons. In the maps, both show that the areas with low biomass were found in the north of the study area while high biomass in the south. Pockets of low biomass were also found in similar locations in the centre. Even though both scatterplots show low R^2 values of 0.13 for the resampled UAS map and 0.09 for the Sentinel 2 map, their patterns of scatter look similar with mostly under-estimation of measured biomass by the models.

4 Discussion

The results presented were both expected and surprising given the knowledge from previous research on biomass with remote sensing, particularly with UAS and how much details they uncovered. Even so, the findings provided fresh insights that warranted further discussion on biomass studies using UAS together with different remote sensing platforms. Before analysing the biomass estimates, it must be stated that the estimates in maps and scatterplots presented before were a representation of the presence (high) or absence (low) of biomass based on Wang's (2006) estimate of maximum and minimum values of biomass in a temperate forest biome of up to 60 kg m^{-2}. This did not represent accurately the absolute values of biomass of the study area in Davert. Nonetheless, the analysis will focus on applying the more accurate UAS estimates to improving satellite estimates.

4.1 UAS as a versatile sensor platform for biomass

The first point of the discussion seeks to answer the first research question posed of the use of UAS in biomass studies. This study has demonstrated that UAS are a versatile sensor platform for biomass studies chiefly because they are able to capture two important components of biomass remotely, which are vegetation indices and elevation on the same day and flight.

In the stepwise regression, the explanatory variables selected of NDVI and Tree Height were satisfactory as they made sense in a botanical context. First, tree height, estimated by the DEM generated from point clouds of the UAS data, had a positive coefficient in the model equation. This means that as tree height increases, so does above ground biomass because the volume of trees increases accordingly, allowing the tree to store more biomass in its stem,

branches, roots and leaves (Goulden *et al*., 1996). This leads to the second variable selected that was NDVI. The NDVI is a measure of green vegetation intensity (Stow *et al*., 2007), and since the UAS images acquired were in the summer month of August, this study assumed that the NDVI recorded was when the maximum foliage grew on trees. In relation to biomass, this also made sense as the higher the NDVI, the higher the presence of green vegetation and hence, higher biomass.

A key aspect of the model was that it showed that tree heights are an important explanatory variable for biomass in all iterations of it (Figure 4 and A2). This is in contrast to previous research that showed including height in biomass estimations does not improve it (Ketterings *et al*., 2001; Soares & Schaeffer-Novelli, 2005). Additionally, the other published equation of biomass estimation with Sentinel 2 by Castillo *et al*. (2017) used in this study also incorporated elevation data from ASTER GDEM. However, the estimates with Sentinel 2 plus ASTER GDEM had a limitation in that the data came from two different sensors where the images captured were not at the same time and resolution.

Thus, the benefits of using UAS in biomass studies, compared to existing satellite based approaches, are that they are versatile, flexible and low cost. This is because they are not only able to capture high-resolution multispectral data from the earth's surface with optical instruments. With the same optical instruments on the same flight, they are also able to capture point cloud data if their flight plans' provide sufficient overlap in images. Nevertheless, data captured by the UAS at high resolutions can be very large to store (nearly 5 GB of raw data were collected for this study area alone) and processing them can be computationally intensive. Hence, using UAS alone to estimate the biomass of a large forest is not practical (Beaumont, *et al*., 2017) and the next discussion point deals with using UAS technology to improve estimates solely by satellites.

4.2 Improving satellite estimates with an adjustment factor

The second point of the discussion seeks to answer the second research question posed of the ways UAS can improve satellite-based estimates. This point is valid since it was shown that the UAS' biomass estimates were the most accurate amongst the four sensors. To improve satellite estimates with UAS requires an adjustment factor applied to the satellite estimates; and one each for World View 3 and Sentinel 2 will be presented.

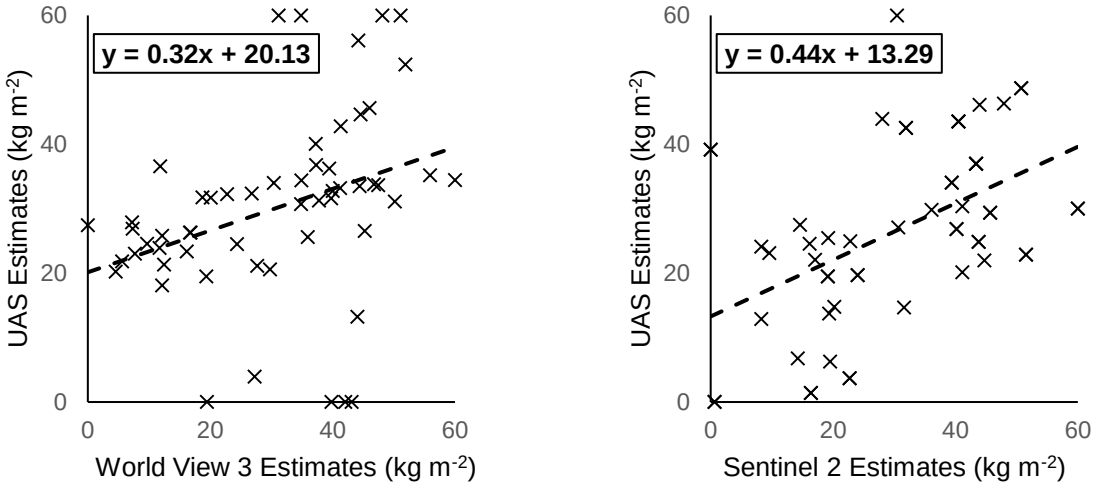

Figure 7: *Scatterplots of satellite estimates against UAS estimates of biomass showing the linearity of the models. The adjustment factor for World View 3 (left) and Sentinel 2 (right) are highlighted above.*

Studies of biomass involving large areas still rely on satellites to cover large swaths of forests for practical reasons mentioned by Shao *et al*. (2017). The alternative of airborne approaches such as Orthophotos and LiDAR flights are expensive to operate (Popescu, 2007) and are not always possible everywhere. Hence, this study argues for the use of UAS to replace on the ground measurements, sometimes referred to as ground truth points, as UAS' estimates are more accurate than satellite estimates and easier to obtain. From the UAS estimates, an accuracy assessment of the satellite estimates can be conducted. Moreover, a satellite specific adjustment factor can be applied to satellite estimates that scales the pixel values of the satellite biomass maps to one that resembles more accurate pixel values from UAS biomass maps.

Two adjustment factors were calculated, one for World View 3 estimates and the other for Sentinel 2 estimates. To calculate the adjustment factors, a simple linear model (Figure 7) was fitted to the explanatory variable of satellite estimates and the response variable of UAS estimates resampled to the respective satellite's resolution. The pixel points sampled were the same 56 points of on the ground measurements. The two equations displayed in figure 7 for World View 3 and Sentinel 2 were the adjustment factors recommended to improve the biomass estimates from the two satellites. To apply this in the context of biomass studies, for example, a patch of forest's biomass estimated by Sentinel 2 can be supplemented by one or more UAS flights over smaller parts of the forest. From the biomass estimates of the more accurate UAS flight, an average of them can be calculated and from the results of the averaged UAS estimates, the adjustment factor for Sentinel 2 can be applied using data from Sentinel 2 and the UAS to improve the overall accuracy of biomass estimates for the entire forest.

4.3 Limitations and further research

First, in terms of data acquired, they were all downloaded from secondary sources and there was no control on what information was collected and how so. This was an important consideration in the formulation of the aims of this research, as work had to be done with what data was available. Nonetheless, studies involving remote sensing of remote areas have relied solely on secondary data sources with visual interpretation of images for accuracy assessments. In this study, data was downloaded not only from remote sensing images but also on the ground measurement of trees collected by NABU. These on the ground measurements (Table A1) were key in building the biomass model and validating estimates.

Second, sensors that capture images in the multispectral range of up to NIR were used in this study. However, there is a growing use of other non-spectral sensor types like Radar (that uses microwave) for vegetation studies (Butnor *et al*., 2003). Radar measurements, especially on airborne platforms, can generate images of high spatial resolution. Moreover, Radar signals are able to penetrate cloud cover, especially for research done in the tropics near the equator where cloud cover constantly obscures satellite images.

Third, in terms of model specificity, the biomass estimation model built was suited for the data collected by the five sensors on the UAS in the context of Davert only. Context specific biomass models was also apparent in the model by Castillo *et al*. (2017) when applied to the Orthophotos, World View 3, and Sentinel 2 sensors even though the sensors had similar radiometry used in their study. This resulted in the low accuracies of the biomass estimates in all the three sensors. This limitation was not address in this study since it is beyond the scope of it, but this problem is common in most biomass studies reviewed. A specific model was built using one sensor in one study area and the model will only be accurate in the context of that study and less so elsewhere. Further research should focus on developing more general biomass estimation models from data acquired from previous research since biomass is found everywhere in the world and research about it is important in mitigating the effects of climate change.

5 Conclusions

In conclusion, this study has achieved its aim and answered the two research questions set forth in the introduction. First, it has demonstrated the use of UAS as a versatile and multi-functional sensor in biomass studies since they are able to capture vegetation indices and elevation data, both important predictors of biomass using remote sensing, in one flight. UAS produced very

high-resolution data that increased the accuracy of biomass estimates, and is not affected by temporal mismatches of spectral and elevation data, a limitation in previous studies. Next, to improve existing satellite-based approaches for biomass estimates, two adjustment factors were suggested, one for World View 3 and the other for Sentinel 2. These adjustments uses relatively accurate UAS estimates of biomass to improve satellite estimates, which covers a larger area that UAS cannot. Nonetheless, caution must be exercised in the interpretation of the values of biomass estimated from this study, as the estimates from UAS are inaccurate in terms of absolute values of biomass per unit area. Rather, they should be regarded as the relative amounts of biomass found in the study site of a typical temperate forest. Future work has been suggested to expand this research to inform studies of biomass estimates using remote sensing techniques and improving biomass estimation models. This study has important implications for research in global biomass estimates and forestry research. Estimations of biomass in inaccessible regions, especially for large areas of forests, still require the use of space or airborne remote sensing techniques, depending on the resources and computational power available. Validation of estimates are also important, and on the ground measurements are not always possible due to forest inaccessibility and researchers should look beyond traditional on the ground measurements of diameter at breast height of trees. The use of UAS should be incorporated in remote sensing studies of biomass not as a wholesale replacement of satellite systems, but rather as a complementary tool for accuracy assessment and improvement of satellite estimates because of UAS' ease of operation anytime, anywhere.

Acknowledgements

Thanks to the DigitalGlobe Foundation for providing the World View 3 image of Davert at no charge. ASTER GDEM is a product of NASA and METI. Thanks to the team at NABU for giving access to on the ground measurements of Davert for this research. Lastly, thanks to Jan Lehmann for operating the UAS in this study.

References

AgiSoft (2016) *AgiSoft PhotoScan Professional: Release 2016*. Agisoft, St. Petersburg.

Avitabile V, Baccini A, Friedl MA, Schmullius C (2012) Capabilities and limitations of Landsat and land cover data for aboveground woody biomass estimation of Uganda. *Remote Sensing of Environment* **117**, 366–380.

Beaumont B, Grippa T, Lennert M, Vanhuysse S, Stephenne N, Wolff E (2017) Toward an operational framework for fine-scale urban land-cover mapping in Wallonia using submeter remote sensing and ancillary vector data. *Journal of Applied Remote Sensing* **11**, 36011.

Boegh E, Soegaard H, Broge N, *et al*. (2002) Airborne Multi-spectral Data for Quantifying Leaf Area Index, Nitrogen Concentration and Photosynthetic Efficiency in Agriculture. *Remote Sensing of Environment* **81**, 179–193.

Brown S, Gillespie AJ, Lugo AE (1989) Biomass estimation methods for tropical forests with applications to forest inventory data. *Forest science* **35**, 881–902.

Butnor JR, Doolittle JA, Johnsen KH, Samuelson L, Stokes T, Kress L (2003) Utility of ground-penetrating radar as a root biomass survey tool in forest systems. *Soil Science Society of America Journal* **67**, 1607–1615.

Cárdenas NY, Joyce KE, Maier SW (2017) Monitoring mangrove forests: Are we taking full advantage of technology? *International Journal of Applied Earth Observation and Geoinformation* **63**, 1–14.

Castillo JAA, Apan AA, Maraseni TN, Salmo III SG (2017) Estimation and mapping of above-ground biomass of mangrove forests and their replacement land uses in the Philippines using Sentinel imagery. *ISPRS Journal of Photogrammetry and Remote Sensing* **134**, 70–85.

Catchpole WR, Wheeler CJ, (1992) Estimating plant biomass: a review of techniques. *Austral Ecology* **17**, 121–131.

Clarke R, Moses LB (2014) The regulation of civilian drones' impacts on public safety. *Computer Law & Security Review* **30**, 263–285.

Congalton RG (1991) A review of assessing the accuracy of classifications of remotely sensed data. *Remote Sensing of Environment* **37**, 35–46.

Copernicus (2016) *Sentinel Data*. Retrieved from ASF DAAC 10 September 2017, processed by ESA.

Crippen RE, (1990) Calculating the vegetation index faster. *Remote Sensing of Environment* **34**, 71–73.

DigitalGlobe (2014) *WorldView-3*. Available at: www.spaceimagingme.com/downloads/sensors/datasheets/DG_WorldView3_DS_2014.pdf (accessed 15 December 2017).

Eckert S (2012) Improved forest biomass and carbon estimations using texture measures from WorldView-2 satellite data. *Remote sensing* **4**, 810–829.

Environmental Systems Research Institute (ESRI) (2016) *ArcGIS Desktop: Release 10.5*, ESRI, Redlands.

European Space Agency (ESA) (2017) *Sentinel-2 MSI Introduction*. Available at: earth.esa.int/web/sentinel/user-guides/sentinel-2-msi (accessed 15 December 2017).

Geoportal NRW (2017a) *Digitale Orthophotos mit 20cm Bodenauflösung paketiert nach Gemeinden*. Available at: www.opengeodata.nrw.de/produkte/geobasis/dop/dop20/ (accessed 10 October 2017).

Geoportal NRW (2017b) *Digitales Oberflächenmodell mittlerer Punktabstand 1m paketiert nach Gemeinden*. Available at: www.opengeodata.nrw.de/produkte/geobasis/dom/dom1l/index.html (accessed 19 October 2017).

Goulden ML, Munge JW, Fa SM, Daub BC, Wofs SC (1996) Measurements of carbon sequestration by long-term eddy covariance: Methods and a critical evaluation of accuracy. *Global Change Biology* **2**, 169–182.

Huete A, Didan K, Miura T, Rodriguez EP, Gao X, Ferreira LG (2002) Overview of the radiometric and biophysical performance of the MODIS vegetation indices. *Remote Sensing of Environment* **83**, 195–213.

Jachowski NR, Quak MS, Friess DA, Duangnamon D, Webb EL, Ziegler AD (2013) Mangrove biomass estimation in Southwest Thailand using machine learning. *Applied Geography* **45**, 311–321.

Jordan CF (1969) Derivation of leaf-area index from quality of light on the forest floor. *Ecology* **50**, 663–666.

Kanemasu ET (1974) Seasonal canopy reflectance patterns of wheat, sorghum, and soybean. *Remote Sensing of Environment* **3**, 43–47.

Kaufman YJ, Tanre D (1992) Atmospherically resistant vegetation index (ARVI) for EOS-MODIS. *IEEE transactions on Geoscience and Remote Sensing* **30**, 261–270.

Ketterings QM, Coe R, van Noordwijk M, Palm CA (2001) Reducing uncertainty in the use of allometric biomass equations for predicting above-ground tree biomass in mixed secondary forests. *Forest Ecology and Management* **146**, 199–209.

Lal R (2004) Soil carbon sequestration to mitigate climate change. *Geoderma* **123,** 1–22.

Oreskes N (2004) The scientific consensus on climate change. *Science* **306**, 1686–1686.

NABU (2017) *Die Davert*. Available at: naturerbe.nabu.de/naturparadiese/nordrhein-westfalen/davert/davert.html (accessed 12 December 2017).

NASA Land Processes Distributed Active Archive Center (LP DAAC) (2015) *Global Data Explorer*. Available: gdex.cr.usgs.gov/gdex/ (accessed 10 September 2017).

Pettorelli N, Vik JO, Mysterud A, Gaillard JM, Tucker CJ, Stenseth NC (2005) Using the satellite-derived NDVI to assess ecological responses to environmental change. *Trends in Ecology and Evolution* **20**, 503–510.

Popescu SC (2007) Estimating biomass of individual pine trees using airborne lidar. *Biomass and Bioenergy* **31**, 646–655.

Rondeaux G, Steven M, Baret F (1996) Optimization of soil-adjusted vegetation indices. *Remote Sensing of Environment* **55**, 95–107.

Rosskopf E, Morhart C, Nahm M (2017) Modelling Shadow Using 3D Tree Models in High Spatial and Temporal Resolution. *Remote Sensing* **9**, 719.

Rouse JW, Haas RH, Schell JA, Deering DW (1973) Monitoring Vegetation Systems in the Great Plains with ERTS. *Third ERTS Symposium* **1**, 309–317.

Scurlock JM, Johnson K, Olson RJ (2002) Estimating net primary productivity from grassland biomass dynamics measurements. *Global Change Biology* **8**, 736–753.

Shao Z, Zhang L, Wang L (2017) Stacked Sparse Autoencoder Modeling Using the Synergy of Airborne LiDAR and Satellite Optical and SAR Data to Map Forest Above-Ground Biomass. *IEEE Journal of Selected Topics in Applied Earth Observations and Remote Sensing* **10**, 5569–5582.

Soares MLG, Schaeffer-Novelli Y (2005) Above-ground biomass of mangrove species. I. Analysis of models. *Estuarine, Coastal and Shelf Science* **65**, 1–18.

Steffan-Dewenter I, Kessler M, Barkmann J, *et al*. (2007) Tradeoffs between income, biodiversity, and ecosystem functioning during tropical rainforest conversion and agroforestry intensification. *Proceedings of the National Academy of Sciences* **104**, 4973–4978.

Stow D, Petersen A, Hope A, Engstrom R, Coulter L (2007). Greenness trends of Arctic tundra vegetation in the 1990s: comparison of two NDVI data sets from NOAA AVHRR systems. *International Journal of Remote Sensing* **28**, 4807–4822.

Tertracam Incorporated (2017) *Mini-MCA: Tetracam's Miniature Multiple Camera Array*. Available at: www.tetracam.com/Products-Mini_MCA.htm (accessed 17 December 2017).

Vexcel Imaging (2016) *Ultra Cam Technical Specifications*. Available at: www.vexcel-imaging.com/products/ultracam-eagle/ultracam-eagle-prime-technical-specs (accessed 17 December 2017).

Wang C (2006) Biomass allometric equations for 10 co-occurring tree species in Chinese temperate forests. *Forest Ecology and Management* **222**, 9–16.

Yang X, Blagodatsky S, Liu F, Beckschäfer P, Xu J, Cadisch G (2017) Rubber tree allometry, biomass partitioning and carbon stocks in mountainous landscapes of sub-tropical China, *Forest Ecology and Management* **404**, 84–99.

Yue J, Yang G, Li C, *et al*. (2017) Estimation of Winter Wheat Above-Ground Biomass Using Unmanned Aerial Vehicle-Based Snapshot Hyperspectral Sensor and Crop Height Improved Models. *Remote Sensing* **9**, 708.

Appendix

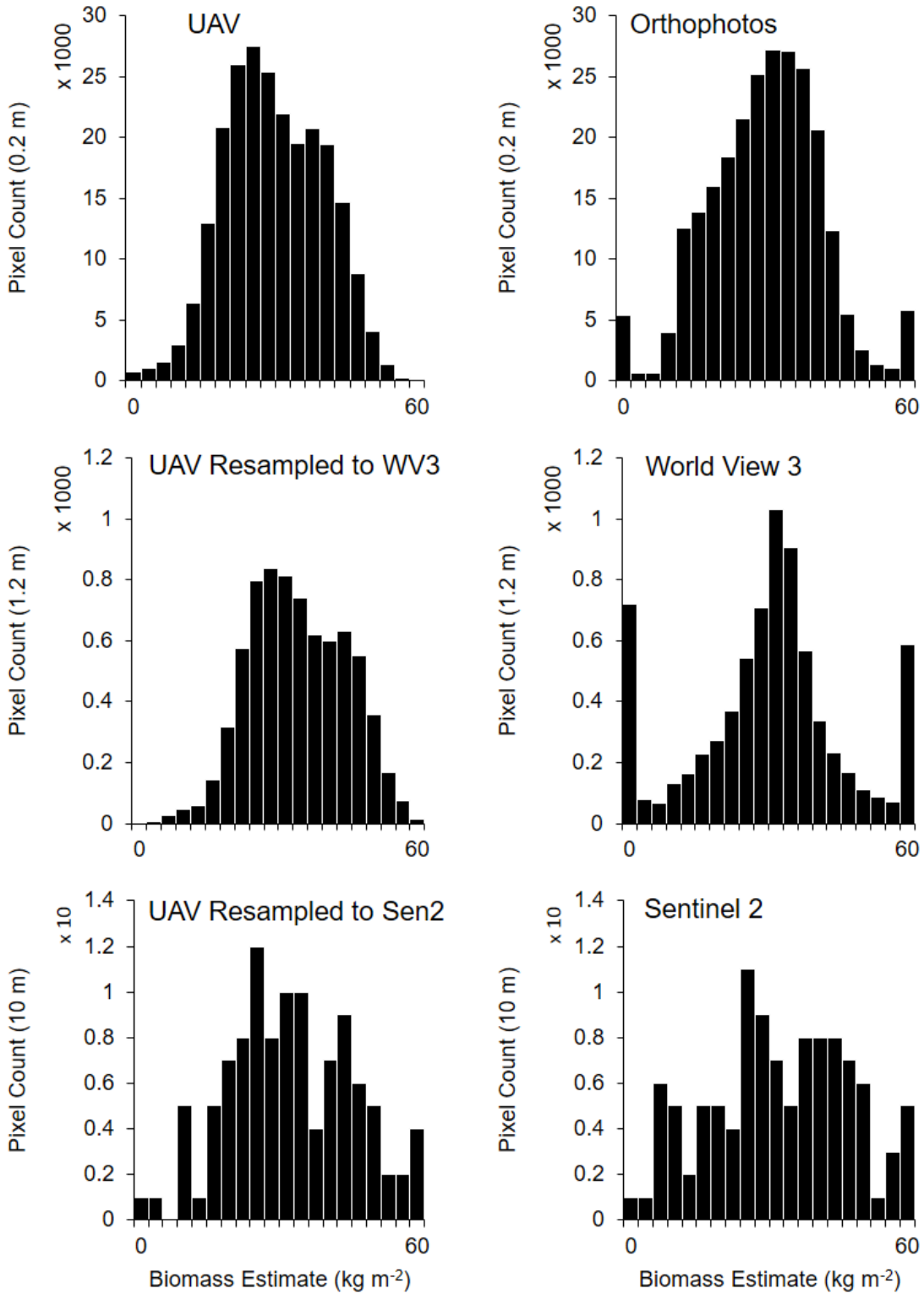

Figure A1: *Histograms of biomass estimates from the different sensors. The comparison here focuses on the distribution of estimates from low to high.*

Model equation

$$Biomass = 13.07 * MARVI + 1.57 * Height - 27.43$$

p value of:	
Model	<0.01
Tree Height	<0.01
MARVI	<0.01
multiple R	0.48
R^2	0.23
Adjusted R^2	0.22
VIF	1.3

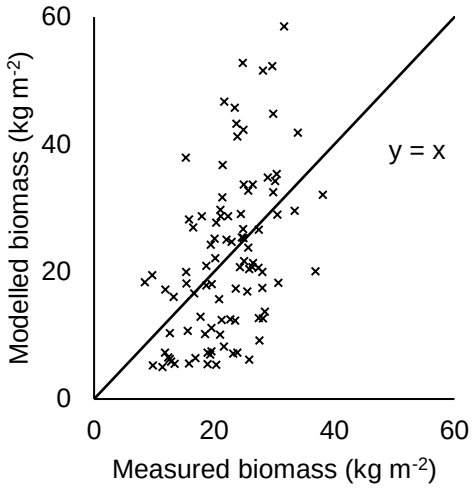

Figure A2: *Biomass estimation model with Red and NIR 2 bands of the UAS (Tetracam Mini-MCA). MARVI was selected instead of NDVI but Tree Height was still an important predictor variable for biomass.*

Table A1: An e*xample of the field measurements collected by NABU. Important to biomass studies area measurements of Genus, Species, DBH and Height.*

Area	Year	Tree No.	Genus	Species	DBH (cm)	Height (dm)	UTM Zone	Easting	Northing
AU3a	2014	1902	*Carpinus*	*betulus*	365	205	32	402968	5745576
AU3a	2014	1870	*Ulmus*	*laevis*	327	207	32	402987	5745565
AU3a	2014	1861	*Fraxinus*	*excelsior*	400	232	32	402983	5745585
AU3a	2014	1864	*Fraxinus*	*excelsior*	403	233	32	402984	5745580
AU3a	2014	1906	*Fraxinus*	*excelsior*	425	237	32	402970	5745579
AU3b	2014	1823	*Fraxinus*	*excelsior*	496	275	32	403038	5745566
AU3b	2014	1812	*Fraxinus*	*excelsior*	511	277	32	403029	5745580
AU3b	2014	1849	*Fraxinus*	*excelsior*	532	280	32	403023	5745571
AU3b	2014	1807	*Fraxinus*	*excelsior*	519	291	32	403026	5745588
AU3b	2014	1819	*Quercus*	*robur*	496	292	32	403035	5745574
AU3c	2014	1913	*Quercus*	*robur*	358	263	32	403014	5745549
AU3c	2014	1942	*Carpinus*	*betulus*	540	271	32	403011	5745520
AU3c	2014	1920	*Fraxinus*	*excelsior*	549	275	32	403021	5745546
AU3c	2014	1939	*Quercus*	*robur*	433	279	32	403015	5745523
AU3c	2014	1944	*Quercus*	*robur*	475	281	32	403012	5745528
AU3d	2014	1767	*Fraxinus*	*excelsior*	403	273	32	403058	5745524
AU3d	2014	1797	*Fagus*	*sylvatica*	513	273	32	403039	5745519
AU3d	2014	1783	*Quercus*	*robur*	527	282	32	403055	5745503
AU3d	2014	1768	*Quercus*	*robur*	514	283	32	403063	5745529
AU3d	2014	1774	*Quercus*	*robur*	572	288	32	403062	5745516
⋮	⋮	⋮	⋮	⋮	⋮	⋮	⋮	⋮	⋮